Pathology - Research and Practice 215 (2019) 586–593

Contents lists available at ScienceDirect

Pathology - Research and Practice

journal homepage: www.elsevier.com/locate/prp

Effects of mesenchymal stem cells harboring the *Interferon-β* gene on A549 lung cancer in nude mice

Xiao Chen[a,b], Kangwu Wang[c], Shijun Chen[d], Yuqing Chen[a,d,*]

[a] Department of Geratology, The First Affiliated Hospital of Bengbu Medical College, Bengbu, Anhui, PR China
[b] School of Medicine, Shandong University, Jinan, Shandong, PR China
[c] Department of Thoracic Surgery, The First Affiliated Hospital of Bengbu Medical College, Bengbu, Anhui, PR China
[d] Department of Respiratory Disease, The First Affiliated Hospital of Bengbu Medical College, Bengbu, Anhui, PR China

ARTICLE INFO

Keywords:
Interferon-β
Mesenchymal stem cells
Lung cancer
Tumorigenicity

ABSTRACT

Interferon-β (IFN-β) exhibits a tumor-killing effect; however, injection of IFN-β alone for lung cancer is often accompanied by side effects. This study investigated the possibility of using umbilical cord mesenchymal stem cells (MSCs) as cellular carriers of *IFN-β*.

Isolated umbilical cord MSCs were transfected with a lentivirus packaging IFN-β-overexpression plasmid. A549 cells were subcutaneously injected into nude mice to establish a non-small cell lung cancer (NSCLC) mouse model. A total of 50 mice were randomly assigned to 5 different groups: a control group, IFN-β group, IFN-β-MSCs group, MSCs-lentivirus group, and MSCs group. Next, the IFN-β-MSCs, MSCs-lentivirus, and MSCs were injected into the A549 lung cancer-bearing mice in the IFN-β-MSCs, MSCs-lentivirus and MSCs groups, respectively. Mice in the control and IFN-β groups were injected with solvent or IFN-β solution. The tumors in nude mice in the IFN-β and IFN-β-MSCs groups grew at significantly slower rates than tumors in the control group, and tumors in the MSCs-lentivirus and MSC groups also grew slowly. The rates of tumor cell apoptosis in the IFN-β and IFN-β-MSCs groups were significantly higher than those in the MSCs-lentivirus and MSCs groups. The livers, lungs, and kidneys of nude mice in the IFN-β group displayed hyperemia, exudation, and pathological lesions, while those of nude mice in the IFN-β-MSCs group showed no abnormal changes. Both INF-β-MSCs and INF-β inhibited the growth of subcutaneously implanted lung tumors; however, INF-β-MSCs specifically targeted the tumor cells, and did not produce the damage to internal organs caused by the use of INF-β alone.

1. Introduction

In recent years, targeted therapy for lung cancer has received a great deal attention by researchers. Some investigators have reported that MSCs can specifically migrate to tumor sites in what is called the homing effect, as demonstrated for glioma, ovarian cancer, and breast cancer [1–3]. MSCs can enter the mesenchyme of these tumors without damaging normal tissues, and thus are considered as the most promising cellular carriers of target genes for the gene therapy of tumors [4,5]. Due to this characteristic of MSCs, we speculated that in the targeted therapy of lung cancer, we could transfect the appropriate tumor suppressor genes into MSCs via lentiviral vectors to inhibit or even kill the tumor cells. If successful, this approach would open up a new path for the clinical targeted therapy of lung cancer.

We selected *interferon-β* (*IFN-β*) as the tumor suppressor gene. IFN-β is a cytokine secreted by fibroblasts, and exhibits a variety of biological activities. It is used to treat certain infections and autoimmune diseases, and also to inhibit the proliferation of tumor cells [6–8]. Researchers studying the treatment of glioblastoma, ovarian cancer, breast cancer, and melanoma [9–12] found that IFN-β can induce the apoptosis of tumor cells and inhibit tumor growth; however, therapies involving the *IFN-β* gene and administered via MSCs for lung cancer are very rare. With respect to problems in the clinical treatment and gene-targeted therapy of lung cancer, we combined the latest research advances at home and abroad, and decided to use umbilical cord mesenchymal stem cells (UCMSCs) as cellular carriers of the *IFN-β* gene in treatment of NSCLC. In this study, the *IFN-β* gene was transfected into UCMSCs (IFN-β-MSCs) by means of lentiviral transfection, and the IFN-β-MSCs were subsequently injected into A549 lung cancer-bearing mice via the tail vein. The tumor sizes in the mouse models were observed, and the lengths of both the long and short diameters of the tumors were measured on a regular basis. Additionally, tumor growth curves were

* Corresponding author at: School of Medicine, Shandong University, Department of Respiratory Disease, The First Affiliated Hospital of Bengbu Medical College, No. 287 Changhuai Road, Bengbu, Anhui, 233003, PR China.
E-mail address: chenyq0552@163.com (Y. Chen).

https://doi.org/10.1016/j.prp.2019.01.013
Received 20 September 2018; Received in revised form 25 December 2018; Accepted 12 January 2019

created, and the effects of IFN-β-MSCs on the growth of lung cancer cells were evaluated. The targeting of tumor tissues by the IFN-β-MSCs was detected using immunofluorescence, and the effects of IFN-β-MSCs on the biological activity of NSCLCs were examined. We also conducted an in-depth exploration of the effects of *IFN-β* gene transfection via UCMSCs on NSCLCs and the possible mechanisms of action involved, with the goal of providing new theoretical foundations and strategies for the gene-targeted therapy of NSCLC.

2. Materials and methods

2.1. Isolation, culture, and passage of MSCs

An umbilical cord (−8 cm in length) from a healthy full-term newborn was immersed in PBS containing 1% penicillin/streptomycin (Beyotime, Haimen, China), and cut into pieces of 2–3 cm in length. The pieces of umbilical cord were then cultured in an inverted T25 cell culture flask containing 2 mL of DMEM/F12 complete medium (Invitrogen, Carlsbad, CA, USA) supplemented with 10% FBS at 37 °C with 5% CO_2; the culture medium was changed every 72 h. When the cells at the bottom of the flask reached > 85% confluence, they were washed 3 times with PBS, digested with 0.25% trypsin (Beyotime), centrifuged at 1500 rpm for 5 min, and subjected to passage at a ratio of 1:2. The MSCs used in this study were in logarithmic growth after 3–5 generations of passage. The umbilical cord sample was acquired with the approval of the Medical Ethics Committee of the First Affiliated Hospital of Bengbu Medical College.

2.2. Phenotyping by flow cytometry

MSCs in their 3rd generation of passage were prepared as single cell suspensions of 1×10^6 cells/mL. After preparation, the serum was discarded, and the suspended cells were transferred into EP tubes (50 μL per tube). Next, 10 μL of each of the above antibodies was added to 40 μL of PBS, which was then centrifuged at 1500 rpm for 5 min. The same types of control antibodies as well as CD90-PE, CD73-PE, CD34-PE, CD105-FITC, CD45-FITC, HLA-DR-FITC, CD14-FITC, and CD19-FITC (eBioscience, San Diego, CA, USA) were added, and incubated at room temperature for 30 min while being protected from light. Next, 1.5 mL of PBS was added to each tube, which was then centrifuged at 1500 rpm for 5 min, and its contents were washed twice. Finally, 350 μL of flow cytometry staining buffer was added to each tube and immunostaining was detected by flow cytometry (Becton Dickenson, Franklin Lakes, NJ, USA). FlowJo software was used to analyze the data.

2.3. Transfection of MSCs with lentivirus

The IFN-β-lentivirus and negative control virus were obtained from Shanghai Jikai Gene Chemical Co., Ltd. (Shanghai, China). A suspension of MSCs with a density of 5×10^4 cells/mL was prepared, and a 2 mL aliquot of the suspended cells was seeded into each well of a 6-well plate and incubated at 37 °C. After 24 h, the medium was discarded and replaced with transfection medium. Transfection of the MSCs with IFN-β gene-lentivirus was performed in accordance with MOI = 15, as determined in a prior experiment; transfection with the negative control virus was performed at MOI = 5. An appropriate quantity of Polybrene was added to the transfection medium, and fresh routine medium was provided after 10 h of transfection. Transfection was then continued for another 72 h, with the cells being changed every 24 h; after which, the transfection was discontinued. The total number of cells (5–7 200-fold fields for each sample were selected by each researcher, with > 700 cells counted) and the number of red fluorescent cells (positive cells) seen under a fluorescence microscope were counted. Next, the average transfection efficiency (number of positive cells/total cell number × 100%) was calculated. Cells with a transfection efficiency > 85% and showing a good growth status were used in subsequent experiments.

2.4. Detection by western blot

Following transfection, cells in the IFN-β-MSCs, MSCs-lentivirus, and MSCs groups were collected, their total proteins were extracted using the protein lysate and BCA method, and the total concentration of IFN-β protein in each group was determined. Next, a 20 μg aliquot of total proteins from each group was separated on a 15% SDS-PAGE gel. The separated protein bands were transferred onto a PVDF membrane, which was then blocked with 5% powdered skim milk for 2 h. Next, the membrane was incubated with rabbit anti-human IFN-β (Abcam, 1:1000) and β-actin (1:500) primary antibodies for 12 h at 4 °C. The primary antibodies were then recovered, and a goat anti-rabbit secondary antibody (Abcam, 1:10,000) was added, and incubated with the membrane at room temperature for 2 h. The immunostained protein bands were then developed with ECL working solution and photographed. The results were analyzed by calculating the ratio of the optical density value of each target band to that of the internal reference (β-actin).

2.5. Enzyme-linked immunosorbent assay (ELISA)

The culture supernatants of MSCs that had been transfected for 24 h, 48 h, and 72 h, respectively, and samples of mouse serum were collected. Next, the concentrations of IFN-β in the collected media and mouse serum samples were detected by using an ELISA kit (Jiangsu Baolai Biotechnology, Yancheng, China) according to the manufacturer's instructions.

2.6. Tumorigenesis in nude mice

Eight-week-old male nude mice (BALB/cJNju-Foxn1nu/Nju) were purchased from the Nanjing Biomedical Research Institute (license No., SCXK [Su] 2015-0001), and A549 human lung adenocarcinoma cells were purchased from the cell bank of the Chinese Academy of Sciences. A549 cells were suspended to a concentration of 1×10^6 cells/mL, and a 1 mL syringe was used to slowly inoculate 0.2 mL of the suspended cells into subcutaneous tissue of the right subcostal tissue of each nude mouse. After being injected, the mice were fed on a regular basis. At 4 days after inoculation, the inoculation sites were observed, and the tumor mass sizes were initially recorded; after which, the lengths of both the long and short diameters of the subcutaneously implanted tumors were recorded every other day. The long and short diameters of each tumor mass were measured as variables "a" and "b", respectively, with a Vernier caliper. Tumor volumes were calculated as $V = ab^2/2$, and the tumor masses were excised and weighed after the nude mice had been sacrificed.

2.7. Group assignments

After the BALB/C nude mice had been subcutaneously injected with tumor cells, they were fed for another 4 weeks. The nude mice were administered drugs via the tail vein in accordance with the following protocol (5 groups): (1) IFN-β-MSCs group (10 mice): 0.2 mL of IFN-β-MSC suspension (1×10^4 cells/0.2 mL) per injection for 5 times, every 2 weeks; (2) MSCs - lentivirus group (10 mice): 0.2 mL of MSCs - lentiviral cell suspension (1×10^4 cells/0.2 mL) per injection for 5 times, every 2 weeks; (3) MSCs group (10 mice): 0.2 mL of MSC suspension (1×10^4 cells/0.2 mL) per injection for 5 times, every 2 weeks; (4) IFN-β group (10 mice): human recombinant interferon β was prepared at a concentration of 100 IU/mL with sterile distilled water, and injected (0.2 mL per injection) for 5 times, every 2 weeks; (5) blank control group (10 mice): A549 lung cancer nude mice without any treatment. The MSCs in each group had been labeled with ERFP *in vitro*.

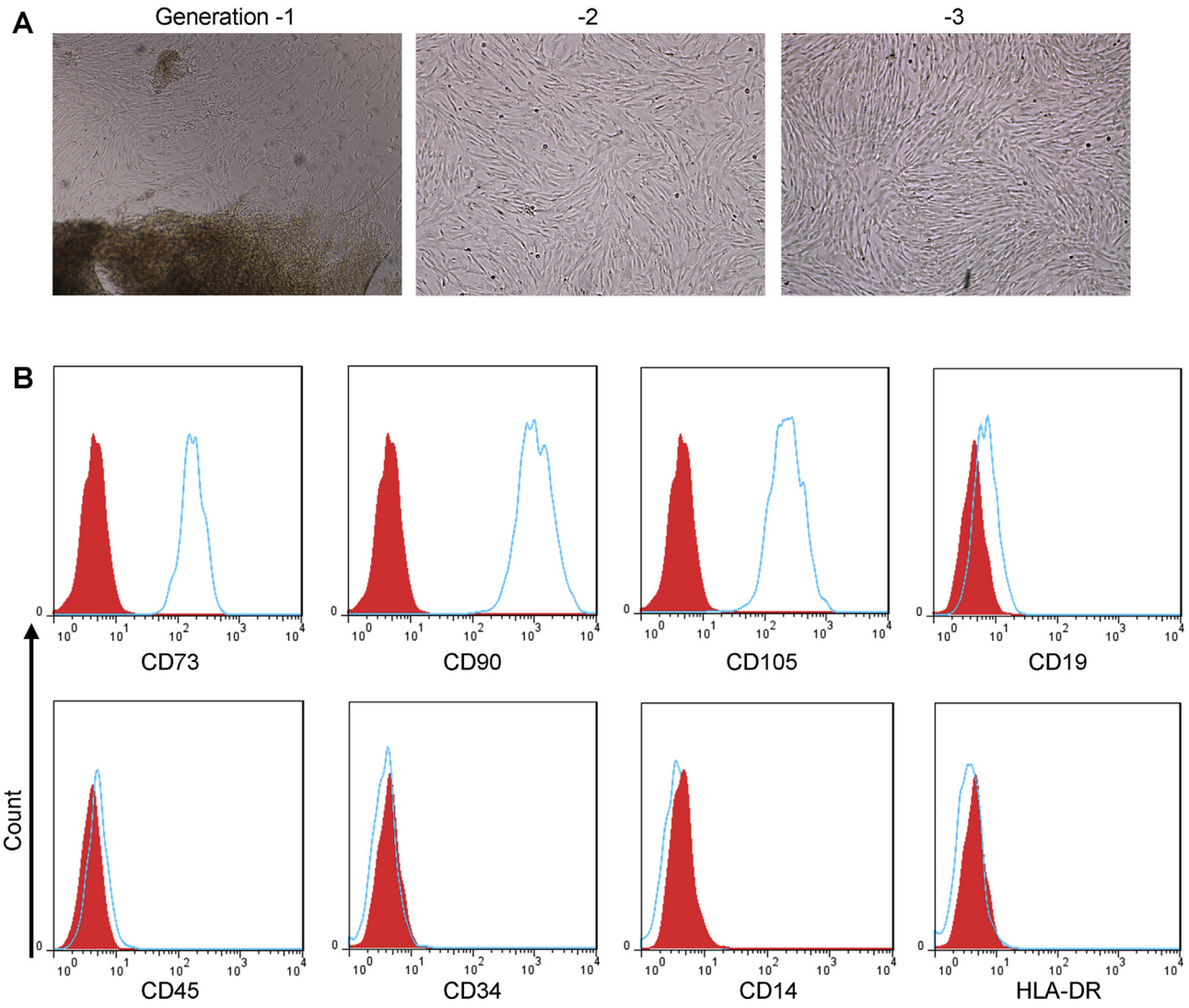

Fig. 1. Isolation, culture, and phenotyping of mouse MSCs.
(A) Growth status of MSCs of Generations 1–3 (Magnification: ×100). (B) Phenotyping of MSCs by flow cytometry.

2.8. H&E staining analysis

Tumors and various organ tissues were removed and fixed with 4% paraformaldehyde for > 24 h. After fixation, the tissues were trimmed, placed in dehydration boxes, and dehydrated with different concentrations of alcohols and xylene; after which, the tissues were embedded in an embedding machine. After trimming the excess paraffin, the tissues were cut into 4 μm thick sections that were de-paraffinized to water. The cell nuclei were stained with Harris hematoxylin for 4˜8 min, differentiated with 1% hydrochloric acid/alcohol solution, turned blue with 0.6% ammonia/water solution, and then washed with water. Next, the sections were stained with eosin for 2–3 min; after which, they were dehydrated with alcohol and sealed with neutral gum. The stained sections were observed under a microscope and photographed for analysis. After staining, the nucleus developed a blue color and the cytoplasm appeared red.

2.9. Tunel staining

Tumor cell apoptosis was detected by use of a Tunel staining kit (Roche Diagnostics, Indianapolis, IN, USA). Paraffin-embedded sections were deparaffinized to water, and a circle was drawn around each tissue with a PAP pen. A drop of proteinase K was placed in the circle, and incubated at 37℃ for 30 min, and then at room temperature for 20 min. Next, the slide holding the tissue was vibrated and cleaned, and then incubated with reagents (Tdt and dUTP) in a Tunel staining kit. After blocking endogenous peroxidase activity, a third reagent (DAB chromogenic solution) was dropped in the circle, causing the positive nuclei to turn brownish yellow in color. Next, the tissues were counterstaining with Harris hematoxylin and differentiated with a differentiation solution (1% hydrochloric acid/alcohol), whereby the ammonia water solution returned to a blue color. The tissue sections were then dehydrated with alcohol and sealed with neutral gum. Five non-overlapping x400 microscopic fields in each tissue section were randomly selected for observation, and the number of apoptotic cells and total number of tumor cells were counted. The apoptotic rate of the tumor cells was calculated as follows: number of apoptotic cells/total number of tumor cells × 100%.

2.10. Immunofluorescence studies

The tumor tissues and samples of liver, lung, spleen, and kidney tissue obtained from all the groups of nude mice were fixed with 4% paraformaldehyde for > 24 h, and subsequently trimmed; after which, they were dehydrated in 15% and 30% sucrose solutions, respectively. The tissues were then embedded in OCT embedding reagent and

sectioned. Next, the tissue sections were fixed in 4% cold paraformaldehyde, cleared in 0.2% Triton X-100 for 10 min, and washed 3 times with PBS. The sections were then blocked for 30 min with serum sharing the same hosts as the secondary antibodies; after which, the blocking solution was placed in a 4℃ wet box overnight with the primary antibodies, and subsequently with secondary antibodies at room temperature for 2 h while being protected from light. The cell nuclei were stained with DAPI for 10 min, washed 3 times with PBS, and subjected to fluorescent photography. The tissue sections from each group were photographed under a fluorescence microscope at x400 magnification, and the photographs were imported into Image-pro Plus software. The relative IOD values of red fluorescence were determined, and the data were exported following an analysis by computer software.

2.11. Statistical methods

IBM SPSS Statistics for Windows, Version 19.0 software (IBM Corp., Armonk, NY, USA) was used to perform a descriptive analysis of the data. Values for continuous variables with a normal distribution are expressed as the mean ± SD. Students *t*-test was used to make comparisons between two groups, and one-way analysis of variance (ANOVA) was used to make comparisons between multiple groups. When individual groups had different mean values for specific parameters, a pairwise comparison q test was performed. A P-value < 0.05 was considered statistically significant.

3. Results

3.1. Isolation, culture, and phenotyping of MSCs in vitro

After MSCs had been cultured for 14 days, the cells were comma-like in shape, and seen to swim outwards under a microscope (Fig. 1A). Upon further culture, the cells became longer and thinner, and their numbers significantly increased. As the number of generations increased, cell growth became more pronounced. The 3rd generation of cells formed colonies with densely radial and vortex-like shapes, and were large in volume and uniform in morphology. The positive expression rates of surface antigens CD90, CD73, and CD105 on the MSCs were 96.3%, 97.5% and 96.9%, respectively, and the negative expression rates of the surface antigens CD45, CD14, CD19, CD34, and HLA-DR were 2.8%, 3.5%, 4.2%, 2.2%, and 2.6%, respectively (Fig. 1B). These data indicated that the MSCs isolated and cultured in this experiment were of high purity.

3.2. Overexpression of IFN-β in MSCs

The fluorescence transfection efficiency in the IFN-β-MSCs and MSCs-lentivirus groups exceeded 85%. The transfected cells displayed a good growth status, and their expression levels of the fluorescence-labeled genes of the target plasmid were normal (Fig. 2A). After the MSCs had been transfected with lentivirus, our detection methods showed that the level of IFN-β protein expression in the IFN-β-MSCs group was significantly higher than those in the MSCs-lentivirus and MSCs groups, and there was no statistically significant difference between the MSCs-lentivirus and MSCs groups (Fig. 2B and C). Furthermore, our ELISA results revealed a high level of IFN-β secretion in the IFN-β-MSCs group (Fig. 2D).

3.3. Inhibition of tumor growth by IFN-β-MSCs

The tumor tissue sections were subjected to H&E staining. Cancer nests were seen in all 5 groups, and various degrees of hemorrhagic necrosis (yellow arrow) were seen in the tumor areas. The disappearance of cellular morphology indicated successful modeling (Fig. 3A). After the lung cancer-bearing nude mice in the 5 groups had been sacrificed at 10 weeks, their tumor tissues were weighed, and the tumor volumes were calculated (Fig. 3B). The inter-group pairwise comparison q-test showed that the tumor weights and volumes of nude mice in the IFN-β and IFN-β-MSCs groups were significantly lower than those in the blank control group, MSCs-lentivirus group, and MSCs group. While the tumor weights and volumes in the MSCs-lentivirus and MSCs groups were increased when compared with those in the blank control group, the differences were not statistically significant. There were no significant differences in terms of tumor weight and volume between the IFN-β and IFN-β-MSCs groups, nor in terms of tumor weight and volume between the MSCs-lentivirus and MSCs groups. The growth curves of tumors in the 5 groups of nude mice (Fig. 3C) showed that the tumors in the IFN-β and IFN-β-MSCs groups grew at a significantly slower rate than tumors in the blank control, MSCs-lentivirus, and MSCs groups. After extirpation of tumor, the weight of IFN-β-MSCs groups' mice was significantly higher than all other groups (Fig. 3D). MSCs attracted into tumor sites were showed by immunohistochemical method CD34 expression (Fig. 3E).

In Fig. 3F, cells with nuclei presenting with brown particles were positive cells, namely apoptotic cells. Large numbers of apoptotic cells were observed in the IFN-β and IFN-β-MSCs groups, and sporadic apoptosis was seen in the other three groups (Fig. 3F and G). The apoptotic rates of tumors in the blank control, IFN-β, IFN-β-MSCs, MSCs-lentivirus, and MSCs groups were 9.32 ± 2.56%, 52.83 ± 7.18%, 50.39 ± 6.02%, 8.79 ± 1.97%, and 9.20 ± 2.18%, respectively. The apoptotic rates of tumor cells in the IFN-β and IFN-β-MSCs groups were significantly greater than those in the blank control, MSCs-lentivirus, and MSCs groups. There was no statistically significant difference between the IFN-β and IFN-β-MSCs groups, or between the control, MSCs-lentivirus, and MSCs groups.

3.4. Gross and pathological observations of various organs, and the ability of IFN-β-MSCs to target tumor cells

H&E staining revealed no abnormal changes in the livers, lungs, spleens, and kidneys of mice in the blank control, IFN-β-MSCs, MSCs-lentivirus, and MSCs groups. There were no obvious abnormalities of the spleens in the IFN-β group, while the livers, lungs, and kidneys in that group had developed hyperemia and various degrees of exudation that were grossly visible. A high magnification microscope (Fig. 4A) revealed some necrotic hepatocytes, hyper-chromatic cytoplasm, nuclear pyknosis, water-like degeneration of hepatocytes, and a few small vacuoles in the cytoplasm. In addition, large numbers of inflammatory cells were seen in the lungs, inflammatory cell foci were seen in the kidneys, and mild glomerular sclerosis was present. The above manifestations indicated that intravenous injection of IFN-β alone had damaged the vital organs of the body to a certain extent; however, such damage was avoided in the IFN-β-MSCs group. Red fluorescence was clearly seen in the tumor tissues of the IFN-β-MSC group (Fig. 4B), signifying that IFN-β was more highly expressed in the tumor tissues than in the normal liver, lung, spleen, and kidney tissues. Furthermore, the serum IFN-β levels in IFN-β-MSCs group were significantly lower than those in the IFN-β group (Fig. 4C). The above results indicate that MSCs can serve as good carriers of the *IFN-β* gene by directly reaching the target tumor cells, and preventing them from entering and damaging other important organs.

4. Discussion

Targeted therapy for lung cancer has become a hot topic in global studies. Some investigators [13,14] found that MSCs can enter the tumor micro-environment *in vivo* via circulating blood, and thereby promote the tumor's growth. However, there are also some investigators who argue differently. In Kaposi's sarcoma, for example, researchers found that MSCs inhibit tumor growth [15], and studies of liver cancer have shown that certain soluble factors secreted by MSCs can inhibit the proliferation of liver cancer cells both *in vitro* and *in vivo*

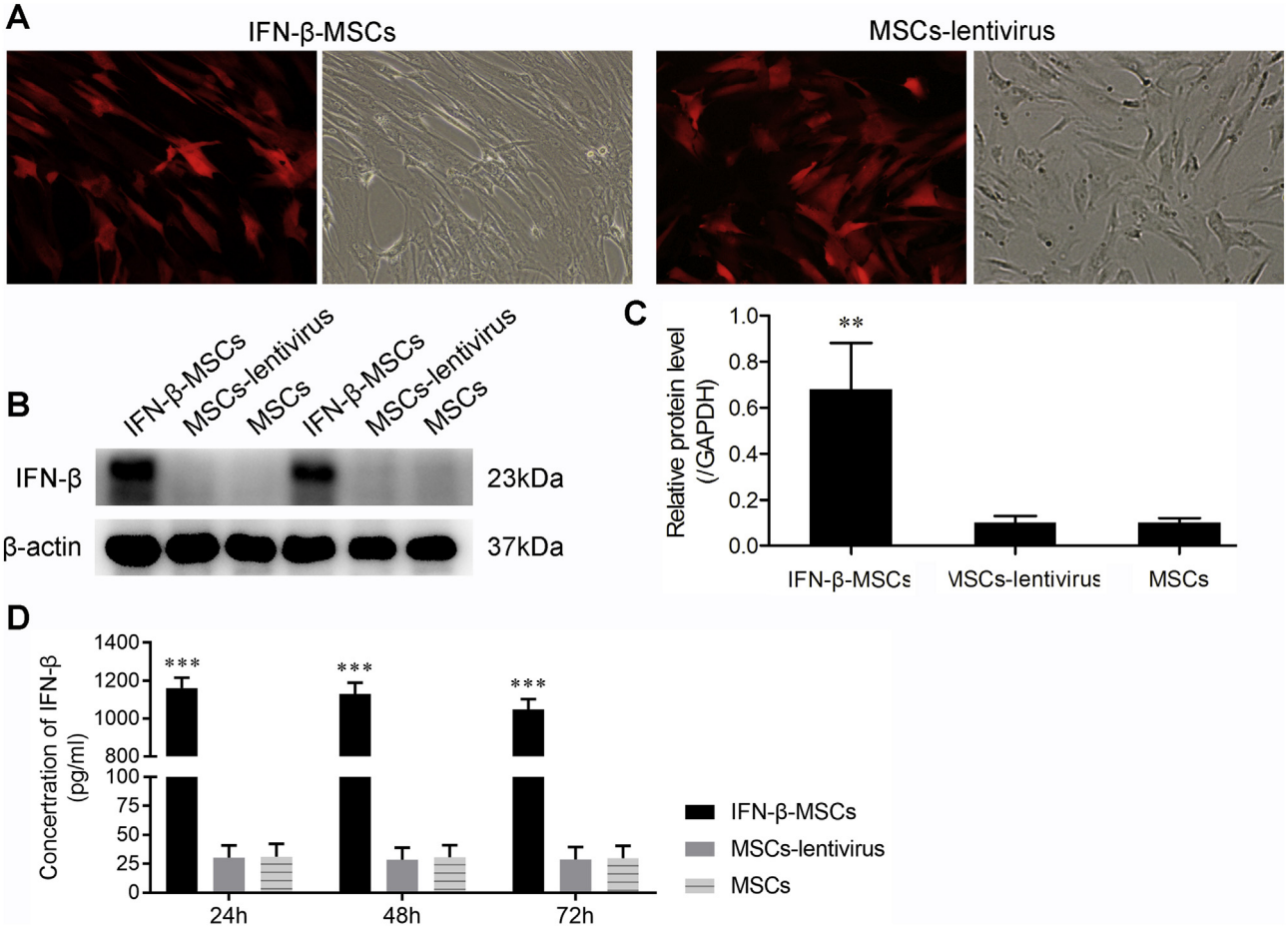

Fig. 2. Overexpression of IFN-β in mouse MSCs.
(A) Transfection efficiency of the IFN-β-lentivirus and blank lentivirus in mouse MSCs. Successful transfection with the IFN-β lentivirus appeared as a fluorescent field, and transfection with the blank lentivirus appeared as a white light field (Magnification: ×200). (B, C) Levels of IFN-β protein expression and comparisons among the groups. (D) Secretion of IFN-β as detected by ELISA.
**P < 0.01, ***P < 0.001, compared with the MSCs-lentivirus group and MSCs group.

[16]. Therefore, it is necessary to thoroughly investigate how human UCMSCs and human UCMSCs transfected with the *IFN-β* gene affect lung cancer cells *in vivo*.

We selected BALB/C nude mice as the animal models for this study due to their following characteristics [17,18]: 1. They exhibit no rejection during xenografting, making them convenient for use in animal experiments on tumors; 2. Human tumor xenografts in nude mice retain their original tissue morphology, immune characteristics, unique karyotypes, and original sensitivities to anti-tumor drugs and ionizing radiation; 3. Human functional tumors transplanted into nude mice can maintain their original functions following transplantation *in vivo*. Therefore, the BALB/C nude mice used in our study were ideal models for investigating human lung cancer. The success rate of modeling was 98%, with one nude mouse dying because of its inability to tolerate subcutaneous inoculation due to weight loss and low food intake. In the IFN-β group, one nude mouse died at 3 weeks after injection of IFN-β via the tail vein. We believe that it died because of low weight, a poor appetite, an unsatisfactory mental status, and an inability to tolerate the side effects of the drug; however, no nude mouse died in the IFN-β-MSCs group. Therefore, we speculated that transfection of the *IFN-β* gene into MSCs could avoid the toxic side effects of IFN-β on organisms.

Nude mice in the 5 different groups were sacrificed at 10 weeks after modeling, and were also assigned to 5 separate groups according to the different drugs administered to the tail vein: the blank control group, IFN-β group, IFN-β-MSCs group, MSCs-lentivirus group, and MSCs group. We excised the tumors from the 5 groups of nude mice, and then weighed the tumors, measured their dimensions, and calculated their volumes. We found that the IFN-β-MSCs and IFN-β groups containing the *IFN-β* gene displayed obvious cancer suppressor effects. Although the MSCs slightly promoted the growth of lung cancer cells *in vivo*, the tumor growth rates in the MSCs group were not significantly different from those in the control group, which might have partially been due to the short survival time of nude mice. Time permitting, we would continue to feed the mice for a period of time and then perform a statistical comparison and analysis. Some studies have shown that the promotion of tumor growth by MSCs *in vivo* is associated with the tumor microenvironment [19–21]. The tumor cells, supporting cells, extracellular matrices, and other factors closely associated with this environment form this microenvironment [22]. Tumor stromal cells play very important roles during tumor cell proliferation and differentiation, making them the most important supporting cells [23]. A lack of nutrition and oxygen are important features of the microenvironment during the process of tumorigenesis; therefore, experts have found that when simulating a lung cancer tumor's hypoxic and ischemic microenvironment via the hunger induction method [24], that MSCs induce autophagy in the lung cancer cells, causing them to resist apoptosis and increase their proliferative capability. Thus when studying the effects of MSCs on lung cancer cells alone, the microenvironment of the tumor cells should be taken into consideration. In this study, we focused on the effects of MSCs harboring the *IFN-β* gene on lung cancer. We found that the IFN-β-MSCs did not contribute to the increase in tumor growth produced by MSCs. In contrast, the IFN-β-MSC group and IFN-β group

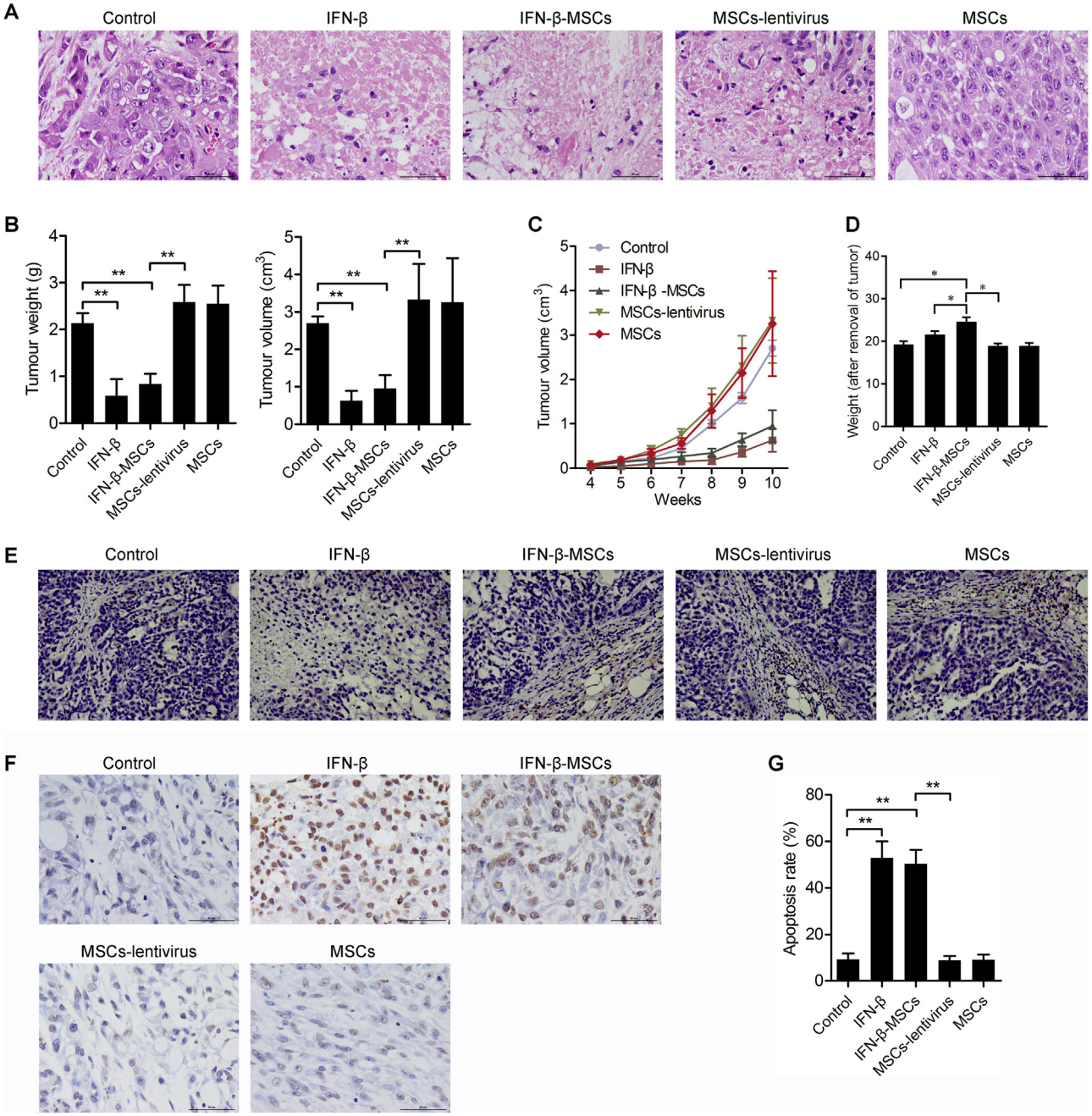

Fig. 3. IFN-β-MSCs inhibited the growth of tumor cells.
(A) Histopathology photographs of the tumor tissues in the nude mice in the 5 groups (Magnification: × 400). (B) Comparisons of tumor weight and volume among the 5 groups. (C) Tumor growth curves for the 5 groups. (D) Weight of mice after excised tumor. (E) $CD34^+$ cells in tumor tissues were showed by immunohistochemistry (Magnification: × 200). (F,G) Apoptotic status of tumor cells (Magnification: × 400). *P < 0.05, **P < 0.01, compared with the control group and MSCs-lentivirus group.

showed similar tumor suppression effects. Based on our Tunel assay results, we speculated that the mechanisms underlying tumor growth inhibition in the IFN-β and IFN-β-MSCs groups were closely associated with the apoptosis of IFN-β-induced tumor cells.

IFN-β exerts a variety of biological functions, and as a member of the host defense system, plays unique roles in inhibiting tumor proliferation and promoting apoptosis [10,25,26]. However, IFN-β has its disadvantages as a treatment for tumors; its short half-life, low dose of systemic tolerance, and numerous side effects limit its clinical applications [27,28]. To avoid systemic adverse reactions and organ damage, we used MSCs as carriers of the *IFN-β* gene. Our subsequent experiments showed that the organs of A549 nude mice in the IFN-β-MSCs, MSCs, and MSCs-lentivirus groups were not markedly damaged, while the livers, lungs, and kidneys of nude mice in the IFN-β group displayed obvious pathological changes. In addition, by using immunofluorescence, we found that IFN-β-MSCs could directly reach their target tumor cells and exert anti-cancer effects. These findings indicated that MSCs harboring the *IFN-β* gene can be administered to avoid the adverse effects of cytokines (eg, IFN-β) on organisms.

5. Conclusion

Our *in vivo* studies with A549 nude mice proved that IFN-β-MSCs can reach lung cancer tumor cells directly, inhibit their growth,

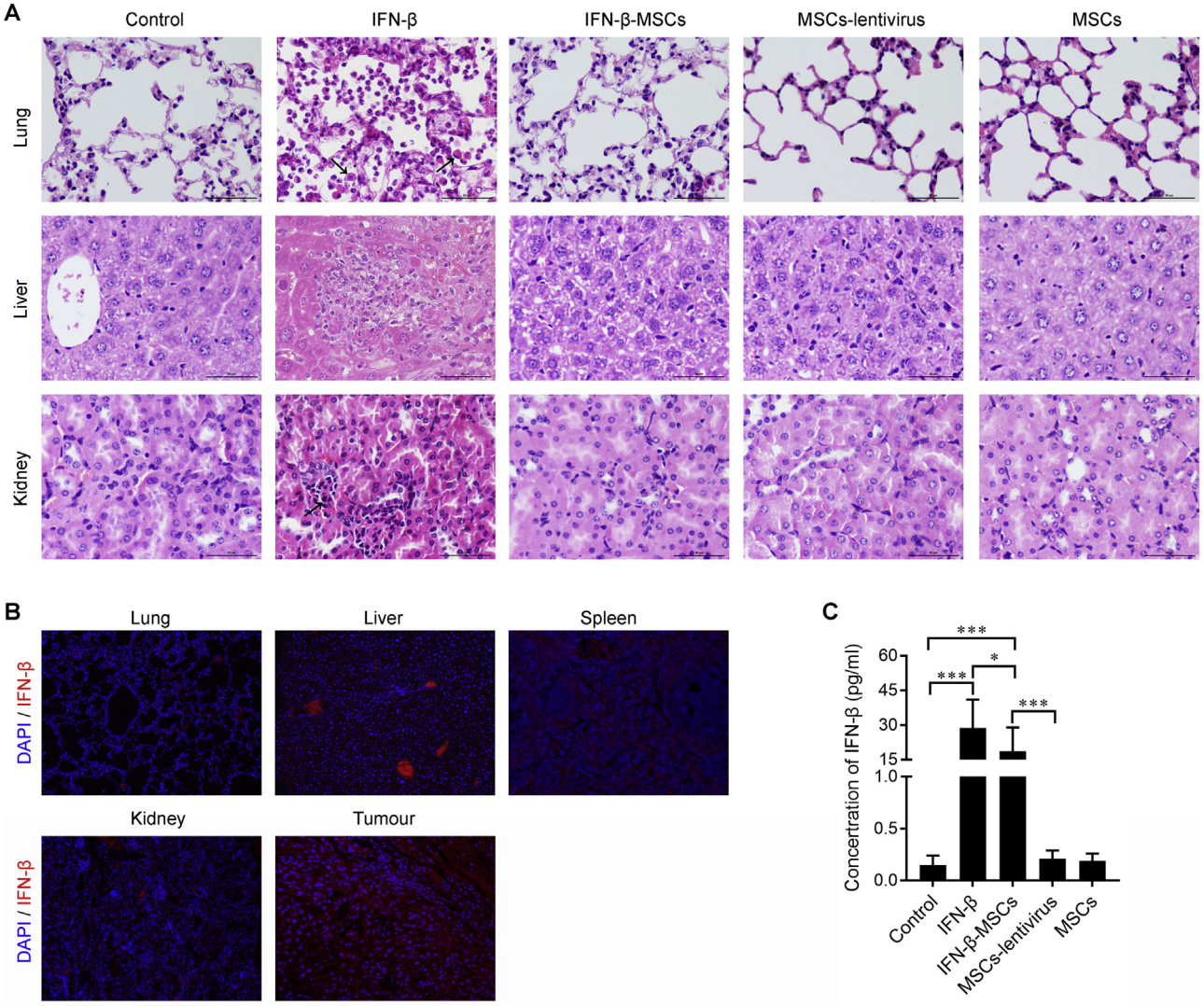

Fig. 4. Targeted inhibition of tumors by IFN-β-MSCs.
(A) IFN-β-MSCs protected normal liver, lung, and kidney tissues from the injuries induced by IFN-β (Magnification: ×400). (B) Expression of IFN-β in the liver, lung, spleen, kidney, and tumor tissues after injection of IFN-β-MSCs (Magnification: ×400). (C) Serum IFN-β levels as detected by ELISA (n = 10). *P < 0.05, ***P < 0.001, compared with the related group.

promote their apoptosis, and avoid the damage to organs produced by administration of IFN-β alone. This research provides a new path for the targeted therapy of NSCLC, and its specific mechanisms merit further investigation.

Competing interests

All authors declare that they have no competing interests.

Funding

This study was supported by the Natural Science Foundation of Anhui Province (1708085QH219) and the Science and Technology Development Project of Bengbu Medical College (No. Byff 12B22; No. Bykf12A16; No. Bykf12B24).

References

[1] B.C.P. Kerrigan, Y. Shimizu, M. Andreeff, F.F. Lang, Mesenchymal stromal cells for the delivery of oncolytic viruses in gliomas, Cytotherapy 19 (2017) 445–457.
[2] T. Chao, G.R. Jiang, Z. Liang, Z.G. Liu, Z.J. Zhu, S.Z. Zheng, A.Y. Wang, L.U. Yin, Mesenchymal stem cells and tumor, Chin. Pharmacol. Bull. 29 (2013) 303–306.
[3] X. Liu, J. Hu, S. Sun, F. Li, W. Cao, Y.U. Wang, Z. Ma, Z. Yu, Mesenchymal stem cells expressing interleukin-18 suppress breast cancer cells in vitro, Exp. Ther. Med. 9 (2015) 1192–1200.
[4] C.X. Zheng, B.D. Sui, N. Liu, C.H. Hu, T. He, X.Y. Zhang, P. Zhao, J. Chen, K. Xuan, Y. Jin, Adipose mesenchymal stem cells from osteoporotic donors preserve functionality and modulate systemic inflammatory microenvironment in osteoporotic cytotherapy, Sci. Rep. 8 (2018).
[5] L. Wu, Y.Z. Zhang, B. Xia, X.W. Li, T. Yuan, C. Tian, H.F. Zhao, Y. Yu, E. Sotomayor, Ibrutinib inhibits mesenchymal stem cells-mediated drug resistance in diffuse large B-cell lymphoma, Chin. J. Hematol. 38 (2017) 1036.
[6] S. Yamamuro, E. Sano, Y. Okamoto, Y. Ochiai, T. Ohta, A. Ogino, A. Natsume, T. Wakabayashi, T. Ueda, H. Hara, Antitumorigenic effect of interferon-β by inhibition of undifferentiated glioblastoma cells, Int. J. Oncol. 47 (2015) 1647–1654.
[7] R.F.V. Medrano, J.P.P. Catani, A.H. Ribeiro, S.L. Tomaz, C.A. Merkel, E. Costanzi-Strauss, B.E. Strauss, Vaccination using melanoma cells treated with p19arf and interferon beta gene transfer in a mouse model: a novel combination for cancer immunotherapy, Cancer Immunol. Immunother. Cii 65 (2016) 1–12.
[8] A. Kakizaki, T. Fujimura, S. Furudate, Y. Kambayashi, T. Yamauchi, H. Yagita, S. Aiba, Immunomodulatory effect of peritumorally administered interferon-beta on melanoma through tumor-associated macrophages, Oncoimmunology 4 (2015).
[9] F. Wolpert, C. Happold, G. Reifenberger, A.M. Florea, R. Deenen, P. Roth, M.C. Neidert, K. Lamszus, M. Westphal, M. Weller, Interferon-β modulates the innate immune response against glioblastoma initiating cells, PLoS One 10 (2015) e0139603.
[10] J.L. Dembinski, S.M. Wilson, E.L. Spaeth, M. Studeny, C. Zompetta, I. Samudio, K. Roby, M. Andreeff, F.C. Marini, Tumor stroma engraftment of gene-modified mesenchymal stem cells as anti-tumor therapy against ovarian cancer, Cytotherapy 15 (2013) 20-32.e22.

[11] B.R. Yi, K.A. Hwang, K.S. Aboody, E.B. Jeung, S.U. Kim, K.C. Choi, Selective anti-tumor effect of neural stem cells expressing cytosine deaminase and interferon-beta against ductal breast cancer cells in cellular and xenograft models, Stem Cell Res. 12 (2014) 36–48.
[12] S.M. Han, C.W. Park, J.O. Ahn, S.C. Park, W.S. Jung, K.W. Seo, J.C. Ra, S.K. Kang, H.W. Lee, H.Y. Youn, Pro-apoptotic and growth-inhibitory effect of IFN-β-over-expressing canine adipose tissue-derived mesenchymal stem cells against melanoma cells, Anticancer Res. 35 (2015) 4749–4756.
[13] M. Devarasetty, E. Wang, S. Soker, A. Skardal, Mesenchymal stem cells support growth and organization of host-liver colorectal-tumor organoids and possibly resistance to chemotherapy, Biofabrication 9 (2017) 021002.
[14] J. Mao, Z. Liang, B. Zhang, H. Yang, X. Li, H. Fu, X. Zhang, Y. Yan, W. Xu, H. Qian, UBR2 enriched in p53 deficient mouse bone marrow mesenchymal stem cell-exosome promoted gastric cancer progression via wnt/β-atenin pathway, Stem Cells 35 (2017) 2267.
[15] A.Y. Khakoo, S. Pati, S.A. Anderson, W. Reid, M.F. Elshal, I.I. Rovira, A.T. Nguyen, D. Malide, C.A. Combs, G. Hall, Human mesenchymal stem cells exert potent antitumorigenic effects in a model of Kaposi's sarcoma, J. Exp. Med. 203 (2006) 1235–1247.
[16] L. Qiao, Z. Xu, T. Zhao, Z. Zhao, M. Shi, R.C. Zhao, L. Ye, X. Zhang, Suppression of tumorigenesis by human mesenchymal stem cells in a hepatoma model, Cell Res. 18 (2008) 500–507.
[17] M. Yan, B. Dongmei, Z. Jingjing, J. Xiaobao, W. Jie, W. Yan, Z. Jiayong, Antitumor activities of liver-targeting peptide modified recombinant human endostatin in BALB/c-nu mice with Hepatocellular carcinoma, Sci. Rep. 7 (2017).
[18] C. Manzotti, R.A. Audisio, G. Pratesi, Importance of orthotopic implantation for human tumors as model systems: relevance to metastasis and invasion, Clin. Exp. Metastasis 11 (1993) 5–14.
[19] Y. Zheng, G. Wang, R. Chen, Y. Hua, Z. Cai, Mesenchymal stem cells in the osteosarcoma microenvironment: their biological properties, influence on tumor growth, and therapeutic implications, Stem Cell Res. Ther. 9 (2018) 22.
[20] R. Liu, S. Wei, J. Chen, S. Xu, Mesenchymal stem cells in lung cancer tumor microenvironment: their biological properties, influence on tumor growth and therapeutic implications, Cancer Lett. 353 (2014) 145–152.
[21] Z. Sun, S. Wang, R.C. Zhao, The roles of mesenchymal stem cells in tumor inflammatory microenvironment, J. Hematol. Oncol. 7 (2014) 14-14.
[22] C.M. Rivera-Cruz, J.J. Shearer, M.F. Neto, M.L. Figueiredo, The immunomodulatory effects of mesenchymal stem cell polarization within the tumor microenvironment niche, Stem Cells Int. 2017 (2017) 1–17.
[23] B. Zhang, Y. Hu, Z. Pang, Modulating the tumor microenvironment to enhance tumor nanomedicine delivery, Front. Pharmacol. 8 (2017).
[24] B. Leber, D.W. Andrews, Closing in on the link between apoptosis and autophagy, F1000 Biol. Rep. 2 (2010) 88.
[25] A. Makowska, L. Wahab, T. Braunschweig, Interferon beta induces apoptosis in nasopharyngeal carcinoma cellsviathe TRAIL-signaling pathway, Oncotarget 9 (2018) 14228–14250.
[26] P.M. van Koetsveld, G. Vitale, R.A. Feelders, M. Waaijers, D.M. Sprij-Mooij, R.R. de Krijger, E.J. Speel, J. Hofland, S.W. Lamberts, W.W. de Herder, Interferon-β is a potent inhibitor of cell growth and cortisol production in vitro and sensitizes human adrenocortical carcinoma cells to mitotane, Endocr. Relat. Cancer 20 (2013) 443–454.
[27] E.V. Popova, A.N. Boiko, O.V. Bykova, I.G. Nankina, T.T. Batysheva, Experience of application of Russian biosimilar of interferon beta-1b for treatment of pediatric multiple sclerosis, Zh Nevrol Psikhiatr Im S S Korsakova 116 (2016) 73.
[28] M.J. Payne, K. Argyropoulou, P. Lorigan, J.J. Mcaleer, D. Farrugia, N. Davidson, C. Kelly, D. Chao, E. Marshall, C. Han, Phase II pilot study of intravenous high-dose interferon with or without maintenance treatment in melanoma at high risk of recurrence, J. Clin. Oncol. Off. J. Am. Soc. Clin. Oncol. 32 (2014) 185–190.